

Histological Relationship with High-Resolution Diffusion Kurtosis Imaging in the Cerebral Cortex

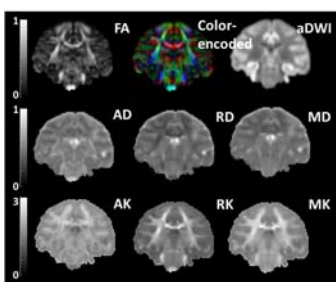
Austin Ouyang¹, Xinzeng Wang¹, Mihovil Pletikos², Nenad Sestan², and Hao Huang¹

¹Advanced Imaging Research Center, University of Texas Southwestern Medical Center, Dallas, Texas, United States, ²Department of Neurobiology, Yale University, New Haven, CT, United States

Target Audience: MR physicists and neuroscientists interested in relationship of high resolution DKI metrics and underlying microstructure

Purpose: The diffusion tensor model assumes Gaussian water diffusion; however, it is believed that water diffuses in a non-Gaussian manner in the presence of diffusion barriers, such as cell membranes and organelles [1-3]. Such non-Gaussian diffusion appears to be more prominent in the cerebral cortex where cellular compartments of neurons and glial cells, neurofilaments and dendrites are widespread. As a relatively new diffusion technology, diffusion kurtosis imaging (DKI) [1] can be used to describe additional microstructural complexities of the tissue and has the potential to characterize the microstructural properties of cerebral cortex. However, the biological meaning of kurtosis metrics of the DKI metrics such as mean kurtosis (MK) or radial kurtosis (RK) has not been delineated so far. The application of relatively high b value in DKI reduces the signal-to-noise ratio (SNR) of the diffusion weighted image (DWI) and makes high resolution DKI especially difficult. On the other hand, to characterize the non-Gaussian diffusion properties of cerebral cortex with only several millimeters of thickness, high resolution DKI is required. In this study, we have successfully acquired DKI data from a postmortem macaque brain with a submillimeter resolution. The high resolution MK map demonstrates clear heterogeneity of non-Gaussian diffusion properties across different cortical regions. Furthermore, by comparison with the corresponding histological image with neurofilament staining, the MK is positively correlated to the neurofilament density.

Methods: High resolution DKI acquisition: A normal postmortem macaque brain was fixed in formalin for over 24 h and later transferred into a custom made plastic tube containing Fomblin for minimal background signal and underwent DKI acquisitions with a 3T Philips Achieva MR system. Two b-values ($b=1500, 4500 \text{ s/mm}^2$) each with 30 independent diffusion-weighted directions [4] were employed to observe the non-Gaussian diffusion properties. Coronal slice acquisitions were obtained using a single-shot EPI sequence (SENSE factor=2). Diffusion weighted imaging parameters were: FOV=130x130x72mm, in plane imaging matrix=144x142, slice thickness=2mm, TR/TE=2100/77.8ms, NSA=24). Two repetitions were performed for each b-value acquisition to further increase the SNR resulting in a total acquisition time of 17 hours. Diffusion tensor and kurtosis fitting: Tensor fitting was conducted with DWI of $b=1500 \text{ s/mm}^2$ by using DTIstudio. With DWI of two b values ($b=1500, 4500 \text{ s/mm}^2$), kurtosis was fitted with in-house Matlab code using DKI constrained linear least squares fits. Parametric map outputs included fractional anisotropy (FA), mean diffusivity (MD), axial diffusivity (AD) and radial diffusivity (RD) from diffusion tensor and axial kurtosis (AK), radial kurtosis (RK), and mean kurtosis (MK) from kurtosis. Quantification of histological image with neurofilament staining: Coronal histological slice of macaque brain stained with SMI-32 was downloaded from brainmaps.org (Jones, UC Davis). SMI-32 staining was used to delineate neurofilaments. MK slice comparison with histology was chosen based on visual inspection of corresponding anatomical features. Histological quantification was completed by the use of computing a structural tensor [5] for every pixel in the image.

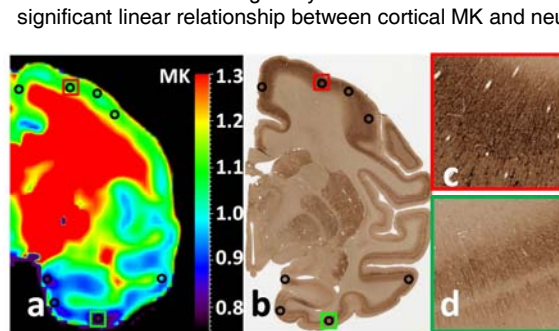
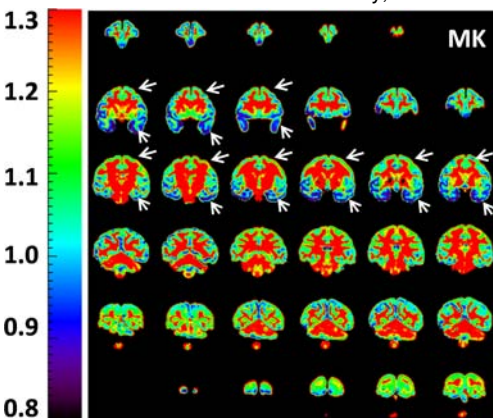


Structure tensors have the ability to characterize fiber microstructures in images along with fiber orientation and anisotropy index (AI) similar to DTI parameters [5] and may help segment fibers from the background. The histology image was first blocked into sizes of 2048x2048 pixels equivalent to 0.9x0.9mm, similar to the DKI image acquisition resolution. A pixel wise structure tensor was computed and pixels with an $AI > 0.6$ were classified as a fiber structure. The ratio of the sum of pixels classified as fiber structure to the blocked area represented the estimated stained fiber density. Correlation between quantified neurofilament density and corresponding MK: MK map was reoriented to be aligned with the histological image. 8 regions-of-interests (ROI) (shown as the black circles in Fig. 3a and 3b) were selected at the frontal and temporal areas. MK values from DKI and neurofilament densities measured from corresponding histological image at these ROIs were correlated to test if there is significant linear relationship between MK and neurofilament density.

Figure 1. DTI and DKI parameters. DTI metrics are in $\mu\text{m}^2/\text{ms}$.

Results: Fig. 1 shows the high resolution maps from DTI-derived metrics and DKI-derived metrics. Specifically, DKI-derived metrics demonstrate high resolution and high SNR to delineate the microstructure of the cerebral cortex. Fig. 2 shows the coronal slices of MK maps. White and gray matter was clearly separated in these MK images. Prominent MK contrast was observed in the coronal slices containing the temporal lobe and the post-, pre-central gyrus, indicated by white arrows. Fig. 3 shows the enlarged MK map at a representative coronal slice and corresponding neurofilament image. It can be observed that higher MK values associated with denser staining (Fig. 3a and 3b). There is a significant difference of MK between frontal and temporal region. For example, the mean MK at the ROIs in the red and green boxes in Fig. 3a are 1.11 ± 0.06 and 0.78 ± 0.07 ($P < 0.00001$), respectively. Correspondingly, the neurofilament densities at the ROIs in the red and green boxes in Fig. 3b are $0.37 \pm 0.02\%$ and $0.21 \pm 0.5\%$, respectively. The apparent difference of neurofilament density in these two boxes can be well appreciated in the enlarged histological images in Fig. 3c and 3d. Furthermore, the linear correlation between MK and neurofilament density at the 8 ROIs in Fig. 3a and 3b is statistically significant ($p < 0.001$).

Discussion / Conclusion: In this study, we have delineated the cortical heterogeneity of kurtosis metrics with high resolution DKI and revealed the



significant linear relationship between cortical MK and neurofilament density with histological image. High MK values correlate directly to a higher likelihood of large diffusion barriers of neurofilament fibers. This may be the first investigation for validating the underlying biological meaning of kurtosis metrics in the cerebral cortex. In the future, various other histological staining methods will be utilized for a more comprehensive validation of kurtosis along with quantification of various other histological features such as cell

density and myelination. The association of DKI metrics obtained noninvasively and quantified histological features could potentially let us better understand the underlying biological meanings of DKI metric changes under the pathological circumstance or during development.

Figure 2 (left): MK maps of all slices. The temporal lobe and post-, pre-central gyrus show the greatest differences (pointed by white arrows). **Figure 3 (right):** (a) MK map, (b) corresponding histological image of neurofilament staining. Enlarged red and green boxes in (b) are shown in (c) and (d).

References: [1] Jensen et al (2005) MRM 53: 1432. [2] Jensen and Helpern (2010) NMR Biomed 23: 198. [3] Wu and Cheung (2010) NMR Biomed 23: 836. [4] Jones et al (1999) MRM 42:515. [5] Budde and Frank (2012) Neuroimage 63:1. **Acknowledgement:** This study is sponsored by NIH MH092535 and NIH EB009545.